SCIENTIFIC REPORTS

OPEN

SUBJECT AREAS:
ENVIRONMENTAL SCIENCES
BIOMATERIALS - PROTEINS

Received
16 September 2013

Accepted
19 November 2013

Published
5 December 2013

Correspondence and requests for materials should be addressed to D.L.K. (david.kaplan@tufts.edu)

Stability of Silk and Collagen Protein Materials in Space

Xiao Hu[1,2], Waseem K. Raja[1], Bo An[1], Olena Tokareva[1], Peggy Cebe[3] & David L. Kaplan[1]

[1]Department of Biomedical Engineering, Tufts University, Medford, MA 02155, USA, [2]Department of Physics & Astronomy, Rowan University, Glassboro, NJ 08028, USA, [3]Department of Physics & Astronomy, Tufts University, Medford, MA 02155, USA.

Collagen and silk materials, in neat forms and as silica composites, were flown for 18 months on the International Space Station [Materials International Space Station Experiment (MISSE)-6] to assess the impact of space radiation on structure and function. As natural biomaterials, the impact of the space environment on films of these proteins was investigated to understand fundamental changes in structure and function related to the future utility in materials and medicine in space environments. About 15% of the film surfaces were etched by heavy ionizing particles such as atomic oxygen, the major component of the low-Earth orbit space environment. Unexpectedly, more than 80% of the silk and collagen materials were chemically crosslinked by space radiation. These findings are critical for designing next-generation biocompatible materials for contact with living systems in space environments, where the effects of heavy ionizing particles and other cosmic radiation need to be considered.

There is little known about the impact of environmental factors in outer space on fibrous proteins, including electromagnetic radiation, high energy particles, and extremes of heat and cold[1–3]. The fibrous proteins, such as collagen, dominate human tissue structure and function[4–7], and the silk fibrous proteins are the most mechanically robust and intriguing spun materials in nature[8–10]. This family of materials is also used in textiles and as medical devices[11–13]. Thus, there is broad interest in understanding how these materials respond in space as a prelude to their future utility in space-related applications due to their broad impact on human health, their environmental and bio-compatibility, and their versatile utility in foods, medicine, and materials.

The primary sequence of collagen involves a GXY amino acid repeat, where G is Glycine, and X and Y can be any of the amino acids but most often are proline and hydroxyproline[14]. Collagen forms macromolecular hierarchical structures, starting from three left-handed helices intertwined to form a right-handed triple helix. Proline and hydroxyproline stabilize the triple helical structure[5,14]. Collagen biomaterials provide essential roles in tissue regeneration, and are also utilized in drug delivery, biosensors, and biophotonics[4–7]. Thus, knowledge about the interactions between the space environment and collagens would be useful for the health and safety of astronauts, as well as possible collagen-based biomaterials for use in space environments.

Silk fibroin proteins are synthesized by silkworms and formed into fibers with remarkable strength and toughness[8–10]. The primary structure of *B. mori* silk fibroin consists mainly of the repeat sequences of $[GAGAGS]_n$, which form physical crosslinks, the beta sheets, which stabilize silk materials[15–18]. Silk has been widely used in the textile industry for centuries, and material options have expanded to films, gels, particles, devices, composites and other formats[11–13,15–18] for use as materials for tissue regeneration. These biomaterials offer tunable mechanical properties and degradability as well as biocompatibility. Understanding the impact of space radiation on silk materials would provide insight into the potential utility of this tough protein-based material for space-related materials and biomedical needs, as well as afford a comparison of very stable beta sheet crystals in silk to the relatively less stable triple helical structure in collagen.

Silica (SiO_2) particles were also incorporated into the protein films (silk-silica, collagen-silica) as examples of organic-inorganic composites to compare responses with the neat protein systems. Silica-related composites are common in many biological systems as well as in artificial composites, and offer potential utility in space-related material systems[19–21]. Silica is widespread in biological systems to support and protect single-celled organisms, such as diatoms, as well as in higher plants and animals[19–21]. In nature, the biosynthesis of biosilica *in vivo* occurs under mild ambient physiological conditions[19], and silica in protein materials can be utilized in osteogenesis related to bone repair[19–21]. Studies on these composite materials can provide information about inorganic-protein interactions in harsh space environments, which can be used for future material designs and medical applications.

Space radiation includes variable in-transit energies such as electromagnetic waves or high-energy particles (Figure 1a)[1–3], and is classified as either ionizing or non-ionizing. Ionizing radiation (energy above ~10 eV)

includes electromagnetic radiation, from reactive X-rays and gamma rays, and cosmic rays which are high energy charged particles. About 99% of the charged particle radiation comes from protons, alpha particles (helium nuclei), and other nuclei. Electrons (beta particles) with energies from a few MeV to 10^{14} MeV[1–3] comprise the other 1% of charged particles. Non-ionizing radiation is low energy radiation including visible light, microwaves and radiowaves. The International Space Station (ISS) in low Earth orbit (LEO) maintains an altitude between 330 km and 435 km, which completes 15.50 orbits per day[1–3]. Typically, there are two main sources of such radiation in space in low Earth orbit, solar events (solar winds, solar flares), and cosmic radiation[1–3]. Cosmic radiation is composed of charged particles (ions, electrons) and a set of secondary particles (protons, charged pions, electron-positron pairs, neutrons, gamma rays and X-rays). Secondary particles from cosmic radiation is often more damaging than primary radiation, as secondary particles have lower energy and remain in matter[1–3].

The goal of the present study was to gain insight into the durability of silk, collagen, and their silica composite materials in the LEO space environment (Fig. 1 b,c,d and Supplementary Fig 1) as part of the Materials International Space Station Experiment (MISSE)-6 program. The MISSE-6 program included goals to understand the impact of the space environment (vacuum, solar radiation, atomic oxygen, micrometeorites, thermal cycling) by flying samples on the space station[3]. Although efforts have been made to identify synthetic polymers that can survive in the harsh space LEO environment[1–3], little has been explored with natural polymers. The insights gained by studying changes in natural material features should help in future ground-based simulations to emulate long-term human space activities related to these materials, as well as lay the groundwork for potential utility as green, durable, reusable, and edible materials for future long term sustainable space travel needs.

Results

Morphology analysis. Post-flight protein samples were analyzed along with control (earth bound) samples. Macroscopic morphology before and after space travel were compared (Figure 2 a,b). The space-traveled silk proteins (Fig. 2a) yellowed (they were originally optically transparent without color), and space-traveled collagen proteins (Fig. 2b) became white (originally transparent without color) compared with the control (earth bound) samples. This change in visual appearance suggested partial degradation or structural changes due to exposure to space radiation. In addition, all neat space silk samples had cracks and had broken into pieces due to the space exposure, suggesting brittleness and loss of structural cohesion. The space collagen samples had a significant decrease in thickness (~20%), suggesting etching damage over 18 months. However, the collagen and the silk composite samples from space exposure (silk-silica, collagen-silica) remained generally intact in morphology and size.

To understand the cause of the changes in morphology, SEM was used to analyze sample surfaces. For controls no significant changes were observed (5 μm × 5 μm surface) (Fig. 2 a,b), and only normal, small aggregates (100 nm to 1 μm) from the silk or collagen materials appeared on the surfaces of the films[22,23]. However, silk and collagen samples from space exposure were covered by "forest-like" fibril networks, with typical domain sizes of 500 nm to 2 μm. Collagen surfaces after space exposure showed similar network morphology, but the fibrils were more connected, with lengths up to 5 μm. Small collagen fibrils could also be observed on the edge of each domain. These features may be due to the combinations of twisted triple-helix structures formed in collagen films[23]. To better understand these surface features, oxygen plasma experiments were conducted on earth to characterize the effects of the atomic and ionized oxygen gases on these natural polymers. Here we used ion

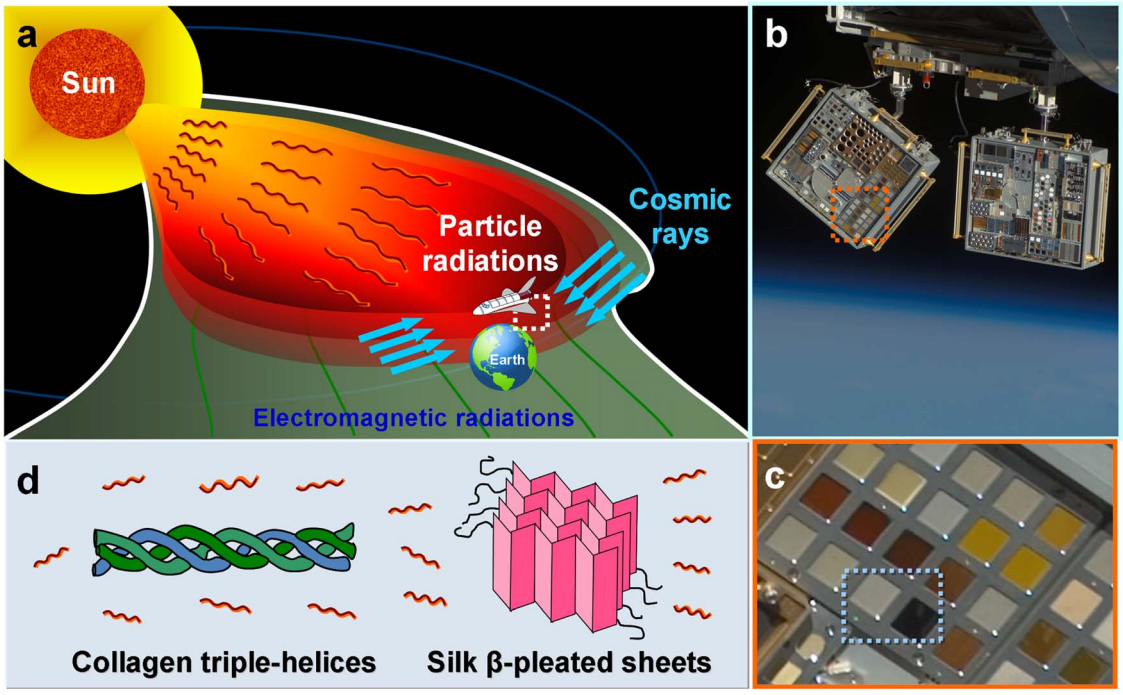

Figure 1 | (a) Materials International Space Station Experiment-6A and 6B (MISSE-6) was used for testing the effects of exposure to the space environment on small samples of various materials including native silks, native collagens, denatured collagens, and their related composite materials etc. (b) Silk and collagens and their composite samples were fixed into several passive frames on MISSE-6 sample box, attached to the outside of the International Space Station. (Photo credit: www.NASA.org) (c) Silk and collagen samples tested in the space are 1″ square with thickness less than 1/8″ (Photo credit: www.NASA.org). Each space traveled sample has several control samples remaining on earth (25°C, dry air environment). (d) After nearly 18 months (2008 ~ 2009) of exposure in the low-Earth orbit space environment, samples were returned to Earth, and long term space environment impacts to protein samples including silk (beta-sheet structure) and collagen (triple-helix structure) proteins were evaluated.

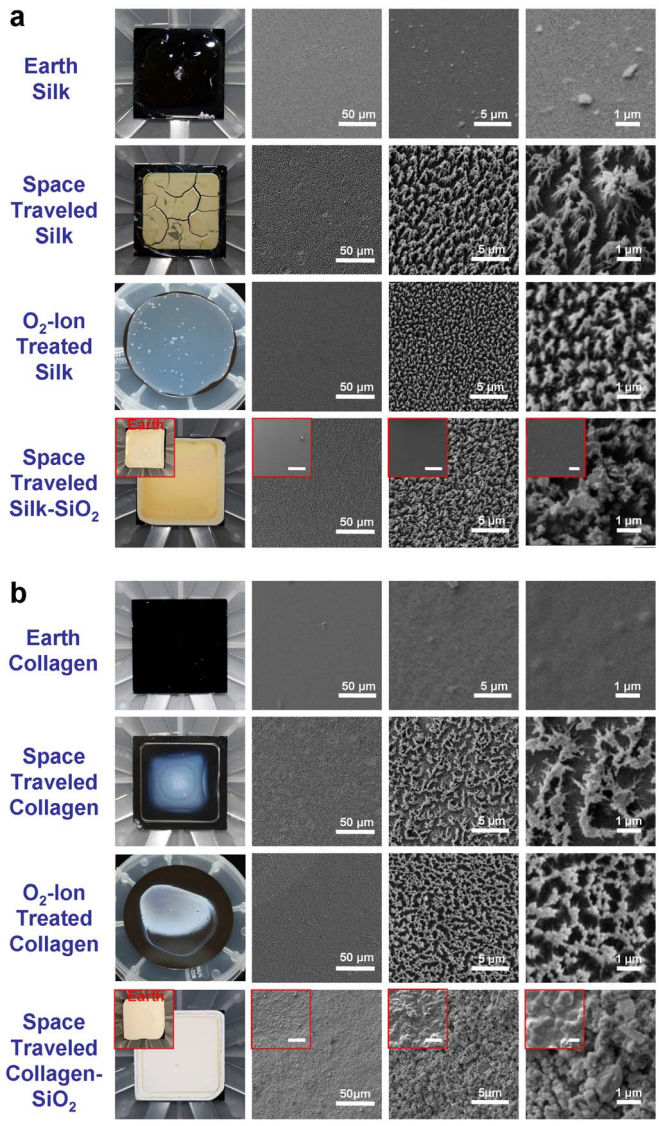

Figure 2 | The color, size, and surface morphology differences in micro- or nanometer scale between protein samples before and after space travel were compared, for (a) silk proteins and silk-silica composites, and for (b) collagen proteins and collagen-silica composites. SEM was used to examine surface morphology change of silk and collagen samples. Space-traveled silk and collagen samples show clearly different surface features, with etched fibril networks. Strong oxygen plasma was also used to compare with the ionizing radiations in the outer space, forming similar but smaller fibril domains on surfaces of control samples.

etching tool (reactive ion etching: RIE) with a high energy to study the effect of oxygen on silk materials within a short time. Typically, the impact energy of atomic oxygen on the material surface in the LEO environment is approximately 5 eV[1–3], but the plasma tool had energy up to 100 eV, which can erode the silk materials much more quickly than samples exposed during 18-months in the LEO environment. Various levels of oxygen plasma were tested on the control samples and the surface topographies observed were similar to the surface patterns on the samples exposed in space. It was also found that when the power of the plasma increased, reactive ion etching tools can strip away the material surface at a higher rate (Supplementary Figure 2). Optimum topography features were observed at around 120 watts for 600 seconds of continuous etching with a etch rate of 0.2 μm/minute. SEM images illustrate that both neat silk and collagen surfaces were etched by the ionized oxygen particles resulting in fibrillar networks, similar to those observed on the samples from space exposure, and the density and size of fibrillar networks on the RIE etched samples increased with the increase of the plasma power (Supplementary Fig. 2); silk fibril "trees" were generally 300 nm to 800 nm in diameter, while the collagen networks were denser with more links than found in the samples from space exposure. The domain thickness was also smaller, around 200 to 700 nm. These results support the finding that space radiation, especially heavy ionizing particle radiation (*e.g.*, atomic oxygen in the LEO space environment), can significantly damage silk and collagen protein material surfaces, in a manner similar to that seen in synthetic polymers[24–29]. In addition, silk-silica and collagen-silica composite materials were compared before and after space travel (see Figure 2(a), 4th row, and Figure 2(b), 4th row). The silk and collagen samples from space exposure were yellower than the control samples and had rougher surfaces than the controls, with many small particles/aggregates together with silica particles at the 5 μm × 5 μm scale, based on SEM analysis. However, these changes in surface morphology were not as pronounced when compared with the neat (unfilled) protein samples. This difference suggests that the silica particles provided some protection for the proteins from radiation damage. The long-term impact of space radiation on silica is complicated[24,25]. Short term exposure of silica materials in the space environment has little impact in terms of damage to physical properties[25,26]. Indeed, SiO_2 coatings have been suggested to protect surfaces of synthetic polymers subjected to the LEO space environment[26]. In addition, the ameliorative effects of silica as an inorganic filler-additive in different synthetic polymers has been reported in space radiation experiments[27]. Silica can act as an efficient excitation-energy sink and also serve to add structural integrity to the polymeric matrix materials[27–29]. Similar mechanisms could also be involved to improve the durability of the silk and collagen materials.

Cross-sections of the samples from space exposure were examined by SEM and AFM (inserts to Supplementary Fig 3) to identify the percentage of material damaged by the radiation (Supplementary Fig 3). The results indicated that about 10 to 15% of the remaining silk or collagen film surfaces were etched by space radiation. In contrast, based on solubility and biodegradation of samples after space exposure these changes were more pronounced. Table 1 shows the mass residues of samples after exposure in space and control protein samples in different solvents and enzyme solutions after 48 hours of degradation at 37°C. The mass measurements indicated that 100% of the silk control samples dissolved in LiBr solution and XIV-protease enzyme solution after 48 hours, and 100% of the collagen control samples dissolved in acetic acid solution and pepsin-acetic acid (pepsin-HAc) solution after 48 hours[14,15]. However, only about 5.4 wt% and 12.9 wt% of silk samples after space exposure dissolved in the LiBr solution and the XIV-protease enzyme solution, respectively. Similarly, less than 8% and 19% of collagen samples after space exposure dissolved in the acetic acid solution and pepsin-HAc solution, respectively. To better understand the degradation of collagens, matrix assisted laser desorption ionization – time of flight-mass spectrometry (MALDI-TOF MS) was used to analyze the samples (Supplementary Fig 4). After 48 hours of treatment in pepsin-HAc solution, the pepsin digested product of the space-traveled collagen films only had three significant peaks at 17,000 m/z, 34,000 m/z and 69,000 m/z (Supplementary Fig 4b), corresponding to the pepsin enzyme itself (Supplementary Fig 4c). No significant collagen degradation peaks were observed in the high molecular weight spectrum. In contrast, the control collagen film contained additional peaks at 46,000 m/z and 93,000 m/z (Supplementary Fig 4a), which are similar to the molecular weight of Type I collagen solution (Supplementary Fig 4d), indicating the control collagen films were dissolved with retention of high molecular weight[5,6,14]. These results show that most surviving space-traveled silk and collagen proteins after etching were chemically or physically crosslinked by space radiation in LEO,

Table 1 | Insoluble mass residues (wt %) of space and control protein samples in different solvents (after 48 hours at 37°C) (n ≥ 3)

Protein/Method	LiBr Solution	Protease XIV Enzyme Solution	Acetic Acid Solution	Pepsin-HAc Solution
Silk-Earth	0%	0%	/	/
Silk-Space	94.6 ± 2.3%	87.1 ± 1.8%	/	/
Collagen-Earth	/	/	0%	0%
Collagen-Space	/	/	92.3 ± 0.7%	81.2 ± 3.3%

resulting in lower solubility and reduced biodegradability than the control samples on earth. These findings also indicated that heavy ionizing particles, such as atomic oxygen, are not the main contributors to the 80% protein crosslinking, since only 10 ~ 15% of the material surfaces was etched by these particles. Instead, the extreme temperature and vacuum conditions in space along with the non-ionizing penetrating radiation such as UV light in LEO, may penetrate the samples during exposure and may be a major cause of the protein crosslinking. This finding is critical in developing future materials for space needs as well as with regard to potential physiological impact. Even with no visible radiation damage on the skin, health issues due to penetrating radiation need to be considered[1,2,30]. The crosslinking effect due to space radiation has also been found with other polymers, such as synthetic elastomers like neoprene, styrene, natural rubber, and urethane[28–31]. The energy-absorbing aromatic rings in the polymer structure increase the radiation stability by aiding the redistribution of the excitation energy throughout the material. Conversely, aliphatic structures (e.g., alcohols and ethers) in polymers are less resistant to radiation[27–29]. Therefore, proteins such as silk and collagen are sensitive polymeric materials due to the peptide backbone. After initial formation of free radicals, oxygen also enters into the reactions to facilitate crosslinking[27–29].

Structural analysis. Protein structures in the space silk and collagen samples were studied by FTIR to determine secondary structures[32–36]. The Amide I (1700–1600 cm^{-1}) and Amide II (1600–1500 cm^{-1}) regions of the spectra are highlighted in Figure 3 (a, b). Fig. 3(a) shows spectra of silk and silk-SiO_2 samples before and after space exposures. Before space travel, both the silk and silk-SiO_2 samples maintained a random-coil-dominated conformation, centered at 1640 cm^{-1} in the Amide I region[34–36]. After space travel, spectral changes occurred in the Amide I region of the silk spectra, with slight peak increases at 1663 cm^{-1}, 1715 cm^{-1} and 1730 cm^{-1}, related to beta-turns[34–36]. This change in conformation indicates that space radiation affected the secondary structures of the silk, and the macroscopic consequence could be the embrittlement of the films (Fig. 1a). However, no beta-sheet crystal peaks were observed in the spectra (the key beta sheet peak at ~1620 cm^{-1} is absent), which suggests that space radiation did not cause the formation of silk protein crystals. Since silk beta-sheet crystals play the role of physical crosslinks in silk materials, in their absence the crosslinking phenomenon we observed in the space-traveled silk samples were therefore due to chemical processes, and not to changes of secondary protein structure. The spectra in Fig. 3(a) also demonstrated that the silica particles protected the silk structures from effects of space radiation. The secondary structures of the silk-SiO_2 samples tended to be stable (Amide I) before and after space radiation exposure, with only slight changes in side chains (Amide II). Fig. 3(b) also shows spectra of collagen and collagen-SiO_2 samples before and after the space radiation exposure. Compared with the silk samples, the macroscopic structures of both collagen and collagen-SiO_2 samples remained stable after exposure to the LEO space environment, with triple-helical peaks observed (at 1636 cm^{-1} and 1653 cm^{-1})[23], although peak shifts were seen in the side chains (Amide II).

The silk samples were also compared for beta-sheet crystallization time and kinetics[16,18]. Figure 3c shows typical FTIR spectra of the space samples before (0 h) and after 1 h and 24 h treatment with 90% methanol[16]. The silk samples from space exposures still crystallized upon soaking in 90% methanol, a traditional method to induce beta-sheet crystallization in silk[16,18]. The beta-sheet crystallinity of methanol-treated silk samples was calculated from curve fitting of the Fourier self-deconvoluted (FSD) spectrum, which was then used to obtain the time-dependent crystallization data[35,36]. Figure 3d shows the crystallinity change in the space-traveled silk and control silk samples in methanol solution at different methanol exposure times (0.25 to 36 hrs). With increased exposure time, the kinetics of β-sheet crystal formation in the space-traveled samples increased gradually, but more slowly than the control silk samples maintained on earth (Fig. 3d). For the earth control silk samples, the crystallinity increased immediately in the 90% methanol solution, and reached a maximum (~60% crystallinity) after 1 hour. In contrast, the silk samples exposed to space radiation reached about 23% crystallinity after 1 hour, and slowly reached a maximum (~47%) after 3 days in methanol. This shows that the LEO space environment impacted the crystallization ability of the silk protein samples like other globular proteins[37]. During radiation exposure, some protein residues such as the N-terminal, C-terminal, or side chains of charged amino-acids could be modified, which would directly affect the self-assembly process of silk protein chains. In addition, radiation induced chemical crosslinks between space-traveled silk molecules would reduce the mobility of the protein chains, so the folding rate of the silk chains into beta sheet crystals would be decreased during the crystallization process.

Thermal analysis. Thermogravimetric analysis, TGA, was performed to compare the thermal stability and degradation rate of silk and collagen samples before and after space exposure. Figure 4 a,b shows the weight percent change of silk (Fig. 4a) and collagen samples (Fig. 4b), respectively, during heating from room temperature to 350°C. The results indicate that both space-traveled silk and collagen proteins degraded more quickly (lost more mass at the same degradation temperature) than the earth-bound control samples. Significantly, the space-traveled collagen samples were very unstable and lost almost 40% of their weight at 120°C (only ~10% of the weight loss was due to water removal). This result indicated that although the collagen triple helical structures were retained (confirmed by FTIR), their thermal stability was significantly reduced after space exposure, probably due to the change of side chain groups, as mentioned earlier. It is also surprising that both space-traveled silk and collagen samples still had more than 5 wt% bound water in their structures, which was removed (evaporated) gradually during the initial thermal treatment from room temperature to 100°C. Therefore, the bound water was most likely regained by the protein samples after returning to earth atmosphere. Therefore protein-water interactions for collagens exposed in the space environment were maintained. Fig. 4a also shows that space-traveled silk-silica samples had higher degradation temperatures (lost less mass at the same degradation temperature) than the neat space silk samples, indicating that the inorganic-protein interactions improved the stability of materials in the space environment. Collagen-silica composites also showed a similar trend in improved stability (Fig. 4b), when compared with neat collagen proteins. Space-travelled collagen-silica composites have less water content than their

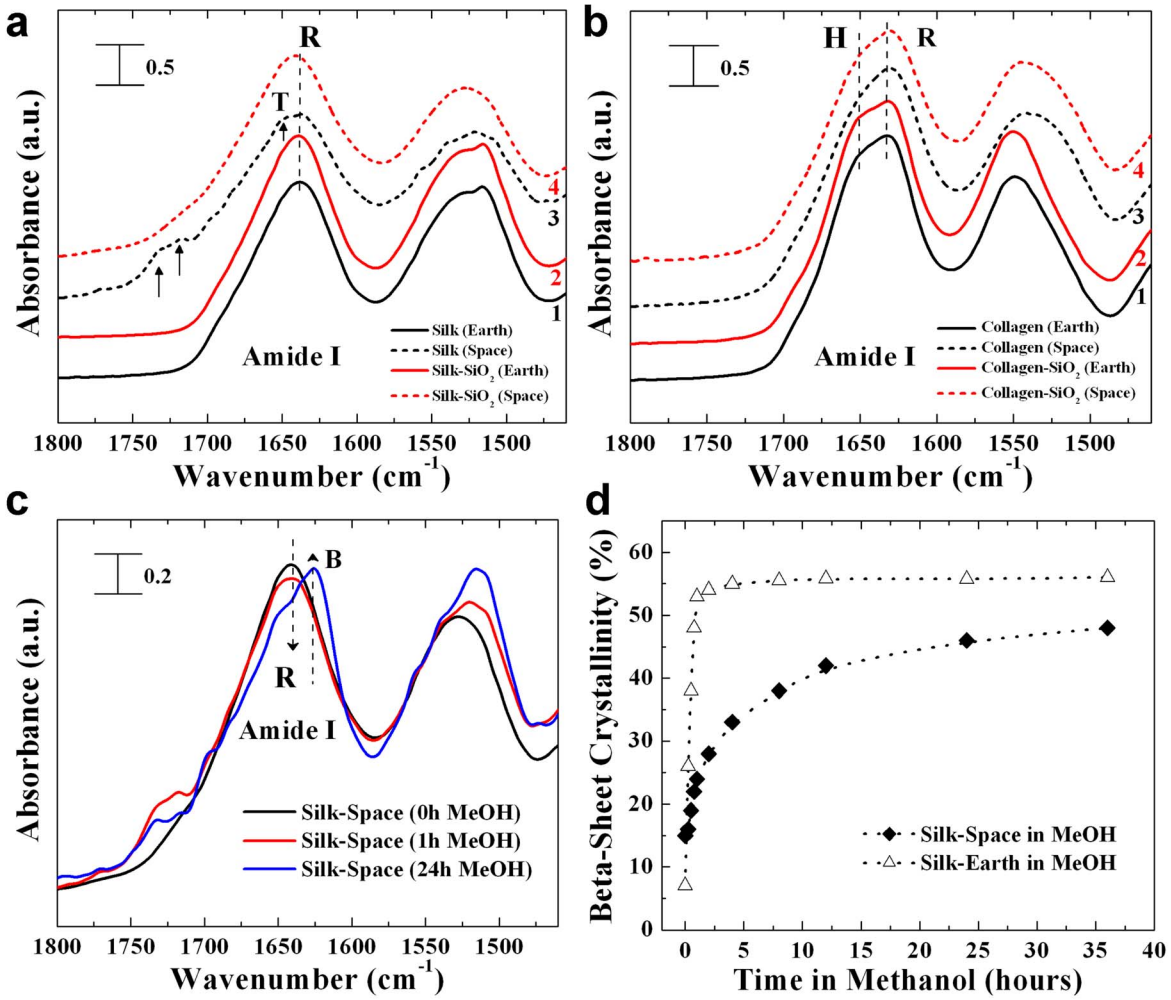

Figure 3 | (a), (b) Amide I (1700–1600 cm^{-1}) and Amide II (1600–1500 cm^{-1}) regions of FTIR spectra were studied to determine the structures of (a) silk and (b) collagen protein samples before and after space trip. (c) Typical FTIR spectrum of space silk sample before (0 h) and after 1 h and 24 h 90% methanol solution treatments. (d) Beta-sheet crystallinity change of space silk and control silk samples in methanol solution at different soaking times (0.25 ~ 36 hours) (symbol sizes have covered the statistical error bars).

controls on earth (4.8% vs. 9.7%), but their high temperature degradation curves (above 270°C) almost overlap.

The glass transition temperatures of the protein samples before and after LEO space exposure were assessed by TMDSC. Fig. 4 c,d shows the reversing heat capacity curves of silk and collagen samples and their silica composites. All samples showed clear heat capacity increments (ΔC_p) during their glass transition temperature regions, indicating occurrence of the conformational change from solid to viscous liquid[36,38]. Generally, silk samples (Fig. 4c) showed a glass transition midpoint temperature around 178°C[36,38], whereas space exposure resulted in a decrease of ~5°C to 173°C. Silk-silica samples had a similar glass transition temperature around 178°C, and space silk-silica samples had almost no change to 177°C, though the ΔC_p changed. This difference suggests that the incorporation of silica particles into the silk materials helped protect the original chains of protein biomaterials, compared with the neat protein samples. The collagen samples (Fig. 4d) showed a glass transition temperature around 204°C, while after space exposure, collagen samples were essential unchanged. Collagen-silica samples had a glass transition temperature around 200°C, and space-traveled collagen-silica samples retained a similar glass transition as well. The glass transition studies demonstrated that all earth-bound control samples had a higher heat capacity increment (ΔC_p) than their corresponding space-traveled samples. The heat capacity increment (ΔC_p) is directly proportional to the average chain mobility, reflecting the number of freely rotating bonds capable of changing the polymer chain conformation[36,38]. A reduction of the ΔC_p indicates that space radiation decreased the average protein chain mobility, such as via the formation of chemical crosslinks, as mentioned earlier.

Discussion

In this study, multiple analyses were performed to understand the impact of the space environment on silk and collagen materials. With nearly 18 months flying in low-Earth orbit on the International Space Station, all protein materials were changed by the exposure to space radiation, but to different degrees depending on the material. Around 10 ~ 15% surface depth of neat silk and collagen films was etched away by ionizing particles such as atomic oxygen in LEO environment, and a similar surface morphology was generated by oxygen plasma etching exposure control experiments on earth. In addition, solubility and enzyme biodegradation studies revealed that more than 80% of the silk and collagen protein chains were chemically crosslinked by penetrating space radiation, causing changes to the proteins. FTIR studies indicated that silk-silica composites or triple-helix structures in native Type I collagens were more resistant to the impact of radiation in space than silk. Although space radiation did not induce beta-sheet crystallization in the silk samples, the ability of these samples to crystallize in terms of rate and maximum

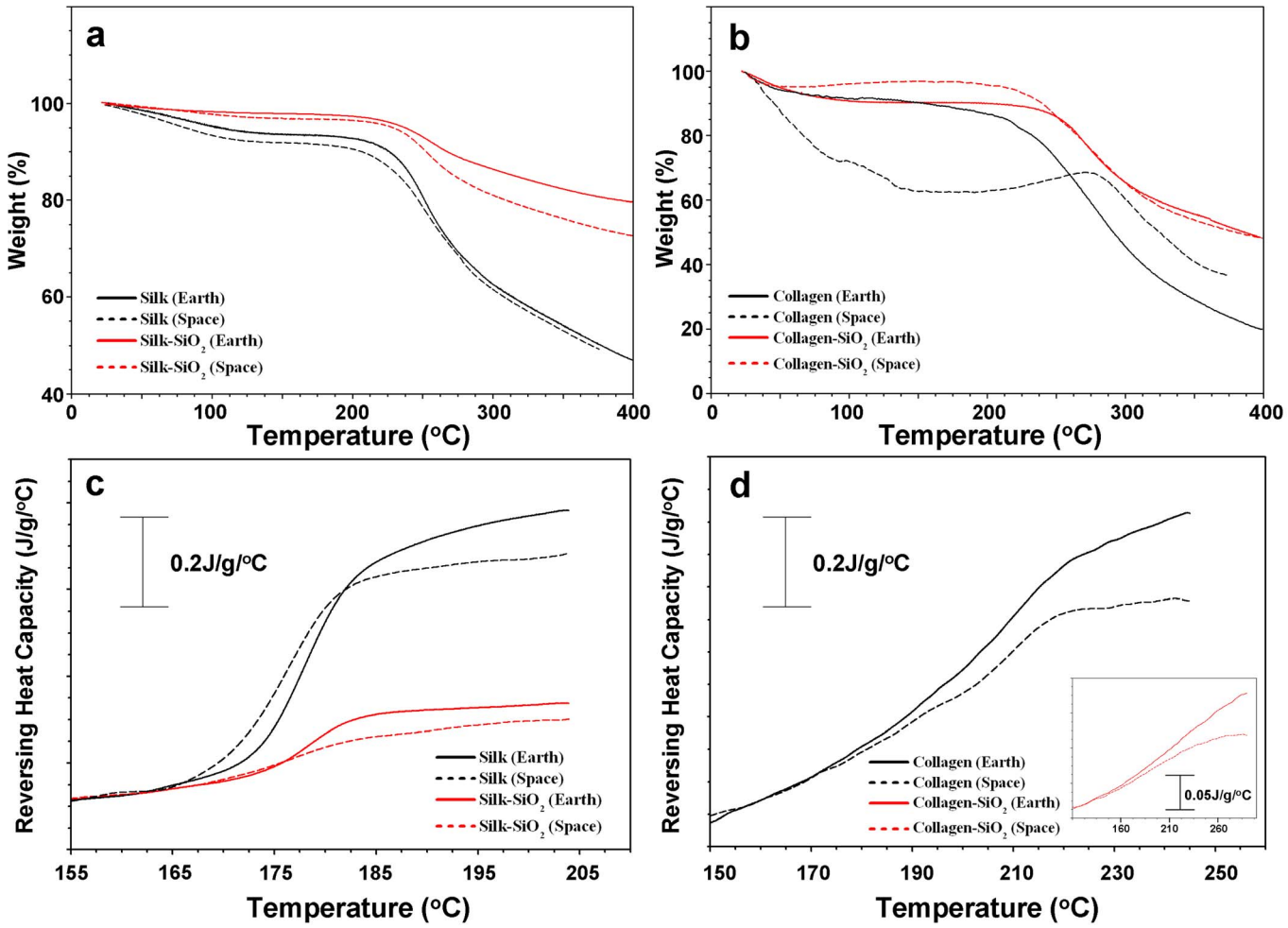

Figure 4 | (a), (b) Weight percentage remaining of silk and silk-silica samples (Fig. 4a), collagen and collagen-silica samples (Fig. 4b) during heating from room temperature to 350°C. (c), (d) Reversing heat capacity curves of silk and collagen samples and their silica composite samples obtained from Temperature-modulated DSC (TMDSC) studies. The heat capacity increments (ΔC_p) during their glass transition temperature regions were highlighted in the figure.

crystallinity was significantly reduced. TMDSC and TGA studies demonstrated that the space environment did not significantly affect the glass transition temperature of the protein samples, while their thermal stability decreased after space travel. These results provide an improved understanding of the durability of various silk and collagen materials in earth orbit, with implications for the design of future materials for various needs during space travel, medical procedures, and physiology. For example, protein-inorganic composites could be an important path forward in designing durable protein materials for space needs, as would protein materials pre-crosslinked on earth to reduce the radiation impact. Further bioengineered protein materials with more aromatic rings in the amino acid side chains could help protect protein materials in the extreme space environments.

Methods

Space mission and sample size. Figure 1 and Supplementary Figure 1 show the Materials International Space Station Experiment (MISSE)-6 space mission program for evaluating long-term space impact on material samples[3]. The Materials International Space Station Experiment-6A and 6B (MISSE-6A and 6B) is a sample box attached to the outside of the International Space Station (also known as Passive Experiment Containers, PECs) and used for testing the effects of exposure to the space environment[3]. The test hardware in the experiment series (MISSE-6A and 6B) launched aboard space shuttle Endeavour (STS-123, the 123th space shuttle flight) in March 11, 2008 (Ref 3 and supplementary references). Following five spacewalks, astronauts Robert L. Behnken and Mike Foreman installed the MISSE-6 on the outside of the Columbus laboratory on Tuesday, March 18, 2008. Samples were retrieved by astronauts Danny Olivas and Nicole Stott during a Sept. 1, 2009, spacewalk. After nearly 18 months of exposure attached to the space station's exterior, the material samples were returned to Earth Sept. 11, 2009 with the STS-128 space shuttle crew that launched on shuttle Discovery from the Kennedy Space Center, USA, Aug. 28, 2009 (Ref 3 and supplementary references). The silk and collagen samples tested were 1″ (2.54 cm) squares with tight tolerances (+0, −0.005″) and the thickness was less than 1/8″ (3.175 mm). Each sample included several control samples that remained on earth (at 25°C, in a dry air environment), which were prepared at same time with the same materials and conditions as the space samples.

Materials. (a) Film Preparation. Cocoons from *B. mori* (supplied by Marion Goldsmith, University of RI, and M. Tsukada, Institute of Sericulture, Tsukuba, Japan) silkworm silk were boiled for 1 h in an aqueous solution of 0.02 M Na_2CO_3 and rinsed with water to extract the glue-like sericin proteins. The extracted silk was then dissolved in 9 M LiBr solution overnight at 37°C and dialyzed (Pierce, Woburn, MA; MWCO 3500 g/mol) against water for 2.5 days[9,12]. Fibroin concentration was determined after evaporation of water overnight and using an analytical balance (Mettler, Greifensee, Switzerland). The concentration was adjusted to 6.7% (*w/v*). One milliliter of the silk solution was transferred onto silicon surfaces (Silicon Valley Microelectronics, CA) and air dried in a fume hood for 4–5 h (native silk, SN). Sterile rat tail derived collagen (Roche, IN) was dissolved at 3 mg/ml in 0.2% acetic acid and maintained in native conformation (CN). Collagen solution (2 ml) was applied on the silicon surface (Silicon Valley Microelectronics, CA) and air dried in a fume hood overnight. **(b) Film Mineralization with Silica.** To prepare silk films with silica (Native silk-SiO_2 films (SNS)), 1 ml of silk solution was mixed with 100 mg of silica powder (0.2 ~ 0.3 μm diameter, Sigma, MO) and applied into the silicon surfaces and air dried overnight as above. Detailed descriptions have been reported previously[20,21]. The same procedure was also used to prepare native (CNS) collagen films with silica.

Oxygen ion stripped films. Reactive ion etching technique was performed to bombard the surface of protein film with charged particles (ionized oxygen). Neat silk

and collagen samples were treated in a modified reactive ion etching tool "March CS-1701F" (Nordon Corporation, Amherst, OH). The samples were treated with oxygen plasma for 600 seconds with a power from 60 watts to 300 watts at two different flow rates of oxygen gas (70 standard cubic centimeter per minute (sccm) and 100 sccm) in the etching chamber.

Etch rate measurements. Profilometer (Veeco Dektak 6M Stylus Profilometer, USA) was used to measure the thickness of etched sample surfaces. Samples were prepared by casting silk films onto glass slides. The dry silk films were half covered by physical masks and were etched for 10 minutes under different conditions. The masks were then removed and the samples were placed into the profilometer and scanned with the stylus tip. The scans were always performed from the untreated area toward the etched area of the films to measure the change of the film thickness. The depths of the etched regions were calculated and etch rates were measured every minute.

Crystallization kinetics of silk films. To understand crystallization kinetics of silk films before and after space trip, variable silk samples ($n \geq 3$ for each condition) were immersed in a 90/10 (v/v) methanol/water solution to induce beta-sheet crystallization of silk[12], and then stored at 25°C. After a designated time, samples were collected and washed by distilled water, and then dried for analysis.

Enzyme degradation. For analysis of radiation-induced crosslinks in the materials, the samples were cut into approximately equivalent mass pieces (~5 to 10 mg, $n \geq 3$ for each condition). The silk samples, were incubated at 37°C in an aqueous solution containing 15.5 U mL^{-1} protease XIV, an enzyme used to assess the degradation of β-sheet crystallized silk samples[16]. In addition, 9 M LiBr solutions were also used to dissolve different silk samples[16]. Collagen samples were incubated in 0.5 M ice cold acetic acids in order to dissolve the films. Pepsin, an enzyme that can dissolve insoluble collagens while cleave denatured collagens into small pieces[5,6], were also used for studying collagen samples. Different collagen samples were incubated in 0.5 M acetic acid with 3,000 Sigma Unit/ml of pepsin (pepsin-HAc solution) at 25°C for the enzyme degradation studies. Solutions were replenished with enzyme each day, and sample residues were collected daily. At designated time points, the samples were rinsed gently with distilled water three times and prepared for mass analysis after collection through centrifugation. Samples without enzyme but in water served as controls.

Differential Scanning Calorimetry (DSC). Thermal transitions of samples were tested by DSC. About 2 ~ 5 mg samples were encapsulated in aluminum pans and heated in a TA Instruments Q100 DSC (New Castle, DE, USA) with a dry nitrogen gas flow of 50 ml/min, and equipped with a refrigerated cooling system. The instrument was calibrated for empty cell baseline with indium for heat flow and temperature. Sapphire reference standards were also used for calibration of the heat capacity. The total heat capacities based on total heat flow, consisting of both the reversing and non-reversing components, were obtained. Temperature-modulated mode DSC measurements were performed at a heating rate of 2 K/min, with a temperature modulation amplitude of 0.318 K/min and period of 60 s. Samples (diameter around 3 mm) were cut from the original films and tested three times for each condition.

Thermogravimetric analysis (TGA). Thermal stabilities and weight changes of samples were tested by TGA. (TA Instruments Q500, New Castle, DE, USA). TGA curves were obtained under nitrogen atmosphere with a gas flow of 50 mL/min. Analysis was first performed by heating the sample from 25°C to 450°C at a rate of 2°C/min. Sample weight loss was recorded as a function of temperature. Each condition was tested three times.

Scanning Electron Microscopy (SEM). SEM was used to assess morphological characterization of the protein samples. The experiments were performed using a Zeiss 55VP System (Oberkochen, Germany). For cross-sectioned surface images, films were first fractured in liquid nitrogen, all the samples were sputtered coated with gold-palladium for SEM imaging.

Atomic Force Microscopy (AFM). AFM was also used to identify the morphological features of the samples. AFM was performed in tapping mode using a Dimension 3100 Scanning Probe Microscope with Nanoscope III and IV controllers (Digital Instruments, Santa Barbara, CA) and equipped with rotated tapping-mode etched silicon probes (RTESP cantilevers with a typical spring constant of 20–80 N/m and a nominal radius of curvature ≤ 10 nm; Nanodevices, Santa Barbara, CA). Both topography and phase signal images were recorded with 512 × 512 data points in ambient air, with a typical scan rate of 1.5 Hz. All samples were put on mica substrates.

Fourier Transform Infrared Spectroscopy (FTIR). To assess structural changes in the samples, Infrared spectroscopy was performed with a Jasco (Easton, MD) FT/IR-6200 Spectrometer, equipped with a deuterated triglycine sulfate (DTGS) detector and a horizontal MIRacle ATR attachment fitted with a Ge crystal (Pike Tech., Madison, WI). Each sample was measured at least 5 times on different spots of the film to confirm spectra. Each measurement incorporated 128 scans from 600 to 4000 cm^{-1} that were Fourier transformed using a Genzel-Happ apodization function to yield spectra with a nominal resolution of 4 cm^{-1}. To deconvolute spectrum with better peak resolution for identifying secondary structures of protein samples, Fourier self-deconvolution (FSD) were performed to obtain peak positions of the Amide I region (1595 ~ 1705 cm-1) using the Opus 5.5 software (Bruker Optics Corp., Billerica, MA, USA), as described previously[34–36]. Each peak was assigned to different secondary structures[34–36]: absorption bands in the frequency range of 1610 ~ 1635 cm^{-1} were assigned to β-sheet structure (B); bands around 1640 ~ 1650 cm^{-1} are related to the random-coil structure (R), bands in the range of 1650 ~ 1660 cm^{-1} represent alpha-helix structure (A), and peaks above 1660 cm^{-1} were ascribed to β-turn structures (T). Finally, the deconvoluted amide I spectra were curve-fitted, and the area ratios of the above assigned bands to the total Amide I area were used to determine the fraction of the secondary structural contents in the films[34–36].

Matrix-Assisted Laser Desorption/Ionization Time of Flight Mass Spectrometry (MALDI-TOF MS). MALDI-TOF MS was used to assess the solubility of collagen sample in pepsin-acetic acids solution. The MALDI matrix was prepared by saturating sinapinic acid (Sigma, MO) in solution containing 50% (v/v) acetonitrile and 0.3% (v/v) trifluoroacetic acid. A 6 μl aliquot of sample solution was mixed with 24 μl of matrix, 1 μl solution was plated onto a 96 spot target plate and allowed to dry. The MALDI-TOF mass spectra were acquired on a Microflex LT system (Bruker Corporation, Billerica, MA) with 50% laser intensity using standard LP (linear positive) 60 kDa method provided by the software.

Statistical analysis. Statistical differences were determined using a Mann-Whitney U test (Independent t-test, SPSS). Statistical significance was assigned as $*p < 0.05$, $**p < 0.01$ and $***p < 0.001$, respectively.

At least three measurements were performed for each type of sample ($n \geq 3$).

1. Cucinotta, F. A. & Durante, M. Cancer risk from exposure to galactic cosmic rays: implications for space exploration by human beings. *Lancet Oncol.* **7**, 431–435 (2006).
2. Blakely, E. A. & Chang, P. Y. A review of ground-based heavy ion radiobiology relevant to space radiation risk assessment: Cataracts and CNS effects. *Adv. Space Res.* **40**, 1307–1319 (2007).
3. Prasad, N. S. & Kinard, W. H. MISSE 6-Testing Materials in Space. NASA Langley Research Center. *Proc. SPIE* **7095**, 70950D (2008).
4. Traub, W., Yonath, A. & Segal, D. M. On the molecular structure of collagen. *Nature* **221**, 914–917 (1969).
5. Brodsky, B. & Persikov, A. V. Molecular structure of the collagen triple helix. *Adv. Protein Chem.* **70**, 301–339 (2005).
6. Maekawa, T., Rathinasamy, T. K., Altman, K. I. & Forbes, W. F. Changes in collagen with age. I. The extraction of acid soluble collagens from the skin of mice. *Exp. Gerontol.* **5**, 177–186 (1970).
7. Hu, X., Cebe, P., Weiss, A. S., Omenetto, F. & Kaplan, D. L. Protein-Based Composite Materials. *Materials Today* **15**, 208–215 (2012).
8. Shao, Z. & Vollrath, F. Materials: Surprising strength of silkworm silk. *Nature* **418**, 741–741 (2002).
9. Jin, H. J. & Kaplan, D. L. Mechanism of silk processing in insects and spiders. *Nature* **424**, 1057–1061 (2003).
10. Hagn, F. *et al.* A conserved spider silk domain acts as a molecular switch that controls fibre assembly. *Nature* **465**, 239–242 (2010).
11. Omenetto, F. G. & Kaplan, D. L. New Opportunities for an Ancient Material. *Science* **329**, 528–531 (2010).
12. Rockwood, D. N. *et al.* Materials fabrication from Bombyx mori silk fibroin. *Nat. Protocols* **6**, 1612–1631 (2011).
13. Hwang, S. *et al.* A Physically Transient Form of Silicon Electronics. *Science* **337**, 1640–1644 (2012).
14. An, B. *et al.* The influence of specific binding of collagen-silk chimeras to silk biomaterials on hMSC behavior. *Biomaterials* **34**, 402–412 (2013).
15. Horan, R. L. *et al.* In vitro degradation of silk fibroin. *Biomaterials* **26**, 3385–3393 (2005).
16. Hu, X. *et al.* Regulation of Silk Material Structure by Temperature-Controlled Water Vapor Annealing. *Biomacromolecules* **12**, 1686–1696 (2011).
17. Wang, Y., Kim, H. J., Vunjak-Novakovic, G. & Kaplan, D. L. Stem cell-based tissue engineering with silk biomaterials. *Biomaterials* **27**, 6064–6082 (2006).
18. Hu, X., Lu, Q., Kaplan, D. L. & Cebe, P. Microphase separation controlled beta-sheet crystallization kinetics in fibrous proteins. *Macromolecules* **42**, 2079–2087 (2009).
19. Wang, X., Schröder, H. C., Wiens, M., Schloßmacher, U. & Müller, W. E. Biosilica: Molecular Biology, Biochemistry and Function in Demosponges as well as its Applied Aspects for Tissue Engineering. *Adv. Mar. Biol.* **62**, 231–71 (2012).
20. Wong, P. F. C. *et al.* Novel nanocomposites from spider silk-silica fusion (chimeric) proteins. *Proc. Natl. Acad. Sci. U S A.* **103**, 9428–33 (2006).
21. Mieszawska, A. J. *et al.* Clay enriched silk biomaterials for bone formation. *Acta. Biomater.* **7**, 3036–41 (2011).
22. Hu, X., Wang, X., Rnjak, J., Weiss, A. S. & Kaplan, D. L. Biomaterials derived from silk-tropoelastin protein systems. *Biomaterials* **31**, 8121–8131 (2010).
23. Rabotyagova, O. S., Cebe, P. & Kaplan, D. L. Collagen Structural Hierarchy and Susceptibility to Degradation by Ultraviolet Radiation. *Mater. Sci. Eng. C Mater. Biol. Appl.* **28**, 1420–1429 (2008).
24. Wittles, M. & Sherrill, F. A. Radiation Damage in SiO_2 Structures. *Phys. Rev.* **93**, 1117–1118 (1954).
25. Primak, W. & Edwards, E. Radiation-Induced Dilatations in Vitreous Silica. *Phys. Rev.* **128**, 2580–2588 (1962).

26. Coia, C., Fozza, A. C., Wertheimer, M. R., Czeremuszkin, G. & Houdayer, A. Radiation-Induced Effects in SiO2 Protective Coatings on Polymeric Spacecraft Materials. *Protection of Space Materials from the Space Environment.* Kleiman, J. I. & Tennyson, R. C. (eds.), 281–290, (Kluwer Academic Publishers, 2001).
27. Rittenhouse, J. B. & Singletary, J. B. *Space Materials Handbook. Third Edition.* (Defense Technical Information Center, 1968).
28. Hanks, C. L. & Hamman, D. J. *Radiation Effects Design Handbook: Section 3. Electrical Insulating Materials and Capacitors.* (National Aeronautics and Space Administration Washington, D.C., 1971).(date of access: 12/15/2012; available website link: http://ntrs.nasa.gov/archive/nasa/casi.ntrs.nasa.gov/19710020300_1971020300.pdf.
29. Mixer, R. Y. & Parkinson, D. B. *The Effect of Nuclear Radiation on Structural Adhesives and Plastics: Part III. Experimental Research.* (Stanford Research Institute, 1957). (date of access: 12/15/2012; available website link: http://contrails.iit.edu/DigitalCollection/1956/WADCTR56-534part03.pdf.
30. Roig, I. *et al.* DNA damage intensity in fibroblasts in a 3-dimensional collagen matrix correlates with the Bragg curve energy distribution of a high LET particle. *Andres. Int. J. Radiat. Biol.* **86**, 194–204 (2010).
31. Hertz, R. M. *et al. Research on Elastomeric and Compliant Materials for Aerospace Sealants.* (Directorate of Materials and Processes, Aeronautical Systems Division, Air Force Systems Command, 1963).
32. Barth, A. & Zscherp, C. What vibrations tell about proteins. *Q. Rev. Biophys.* **35**, 369–430 (2002).
33. Jung, C. Insight into protein structure and protein–ligand recognition by Fourier transform infrared spectroscopy. *J. Mol. Recognit.* **13**, 325–351 (2000).
34. Qin, G., Hu, X., Cebe, P. & Kaplan, D. L. Mechanism of resilin elasticity. *Nat. Commun.* **3**, 1003 (2012).
35. Hu, X., Kaplan, D. & Cebe, P. Determining Beta-Sheet Crystallinity in Fibrous Proteins by Thermal Analysis and Infrared Spectroscopy. *Macromolecules* **39**, 6161–6170 (2006).
36. Hu, X., Kaplan, D. & Cebe, P. Dynamic Protein−Water Relationships during β-Sheet Formation. *Macromolecules* **41**, 3939–3948 (2008).
37. Vergara, A., Lorber, B., Sauter, C., Giege, R. & Zagari, A. Lessons from crystals grown in the Advanced Protein Crystallisation Facility for conventional crystallisation applied to structural biology. *Biophysi. Chem.* **118**, 102–112 (2005).
38. Pyda, M., Hu, X. & Cebe, P. Heat Capacity of Silk Fibroin Based on the Vibrational Motion of Poly(amino acid)s in the Presence and Absence of Water. *Macromolecules* **41**, 4786–4793 (2008).

Acknowledgments

The authors thank the AFOSR (Hugh Delong), the NIH (P41 EB002520, DE017207) and NASA for support of this research. We also thank Boeing and NASA-Langley personnel who managed the MISSE-6 mission in International Space Station, as well as the astronauts involved and mentioned earlier.

Author contributions

X.H., W.K.R., B.A. and O.R.T. performed experiments. X.H., W.K.R., B.A., O.R.T., P.C. and D.L.K. discussed experiments and wrote the paper. All authors analyzed data and commented on the paper.

Additional information

Reprints and permissions information is available online at http://npg.nature.com/reprintsandpermissions.

Supplementary information accompanies this paper at http://www.nature.com/scientificreports

Competing financial interests: The authors declare no competing financial interests.

How to cite this article: Hu, X. *et al.* Stability of Silk and Collagen Protein Materials in Space. *Sci. Rep.* **3**, 3428; DOI:10.1038/srep03428 (2013).